

# Detection of Conductive Objects with Electrical Capacitance Tomography

Stephan Mühlbacher-Karrer, Hubert Zangl  
Institute of Smart System Technologies, Sensors and Actuators  
Alpen-Adria-Universität Klagenfurt  
9020 Klagenfurt, Austria  
Email: stephan.muehlbacher-karrer@aau.at

**Abstract**—We present an Electrical Capacitance Tomography (ECT) based object detection system, which can work with conductive objects. For grounded objects, the coupling to the distant ground is considered in the forward problem by means of coupling conductivities. For the reconstruction of the material distribution within the Region of Interest (ROI) we use a linear Bayesian inversion method in combination with a non-linear artifact reduction. The system achieves a high object detection rate in the ROI and allows to select a subregion of the ROI, where objects should be detected. This is beneficial, e.g., for applications in robot grasper. The proposed light-weight signal processing chain, which has real time capability, allows to integrate this sensing technology on a platform limited in terms of space, energy and computational resources. Satisfying these requirements makes the system suitable for mobile and robotic applications.

## I. INTRODUCTION

ECT is a non-invasive measurement method to determine the material distribution of the ROI, e.g., cross-section of a pipe [1]. In the classical ECT setup, the environment is well known and certain simplifications can be made, i.e. the materials, which may appear in the ROI are usually known in advance. When ECT is applied in the field of proximity sensing using a planar electrode geometry as shown in Fig. 3, usually fewer assumptions can be made about the environment, e.g., external disturber, objects, e.g., the material or coupling to ground and additional sensing effects have to be taken into account, e.g., shielding effect. Thus, the objects may be fairly conductive and may have good connection to distant ground and a so-called leakage current may flow through this connection. The leakage effect has an impact on the measured capacitances and should not be neglected. Thus, the work of [2] has to be extended and the leakage effect [3] has to be taken into account in order to also work with conductive materials. Consequently, our forward model incorporates the physical circumstances by considering the coupling of the object. This extends the classical ECT approach as we consider the leakage effect in the reconstruction as shown in the measurement model in Fig. 2. We combine a light-weight reconstruction algorithm with object detection for leakage distribution. To further increase the robustness of the reconstruction approach (to obtain the leakage conductivity images) it is combined with a non-linear artifact reduction technique. Finally, a hypothesis test is applied on the reconstructed leakage conductivity images to estimate the position of the objects. The benefits of our proposed approach are:

- A position estimation of the object can be realized with



Fig. 1. Application example: An ECT system integrated in the fingers of a robot allows detection and position estimation for objects in the grasping area [4]. Such a system can help to improve the grasping performance.

realtime capability.

- It allows selecting a subregion of the ROI, where objects should be detected, e.g., for robotic grasper applications.
- The detection images can be merged to a one image.

## II. RELATED WORK

According to the application requirements, in ECT a variety of deterministic and statistical reconstruction algorithms can be used, e.g., Linear Backprojection (LBP) [5], Non-linear Iterative (NI) [6], Gauss-Newton schema, Optimal Approximation (OA) [7], Kalman Filters (KF), Markov Chain Monte Carlo (MCMC) [8] methods, etc. In terms of computational effort and image quality of the reconstruction each algorithm has certain advantages and drawbacks. The Bayesian method Optimal First Order Approximation (OFOA) [9] is used in this paper. Bayesian methods provide information about the uncertainty of the reconstruction result, which is beneficial for the hypothesis test used for the implemented object detection. A further advantage of OFOA is a fast reconstruction speed, which is in the category of linear approximation algorithms, e.g., LBP, combined with an increased quality of the reconstruction image. Due to the constraint linear functions of OFOA artifacts may occur due to the non-linear influence of the material on the measurements in regions with low permittivity. To reduce it the non linear Box-Cox transformation [10] is applied to further increase the reliability of the object detection.

## III. SYSTEM DESCRIPTION AND THEORETICAL BACKGROUND

### A. Sensing Principle

Capacitive sensing is based on the interaction of the electric field and an object approaching the sensor front end causing a field deformation. The differential measurement mode is utilized as shown in Fig. 2. In this mode, the capacitance between two electrodes is determined by applying an excitation signal to the transmitter electrode and measuring

the displacement current at the receiver electrode.

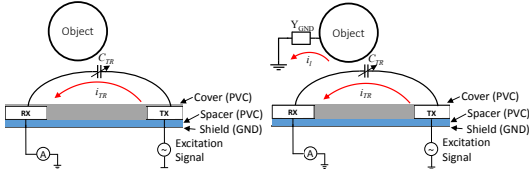


Fig. 2. The differential measurement mode. On the left and right side the approaching object is not well and well coupled to ground, respectively.  $C_{TR}$  depicts the influence of the approaching object changing the capacitance depending on its position.  $i_{TR}$  expresses the displacement current. The leakage current  $i_l$  significantly reduces  $i_{TR}$  at the receiver side resulting in a decrease of  $C_{TR}$ .

### B. Leakage Effect

The leakage effect describes the effect that large objects or objects with a low impedance to distant ground drain displacement current originating from a transmitter electrode towards distant ground (see Fig. 2). This changes the field distribution and thus the measured capacitances. As the coupling paths to distant ground have enormous variability they can not be directly included in the forward map. Instead, the effect is summarized in the leakage currents. In this paper the leakage effect is modeled by  $Y_{GND}$  (see Fig. 2) denoting the object's coupling to distant ground. More precisely, we approximate the object's coupling admittance to ground  $Y_{GND}$  by means of a homogeneous leakage conductivity  $\sigma_l$  with respect to ground over the cross sectional area of the object.

### C. Sensor Front End

Our sensor front end is a Printed Circuit Board (PCB) (see Fig. 3) comprising  $n = 7$  electrodes on the front side and a conductive shield on the rear side. The electrodes are  $12 \text{ mm} \times 152 \text{ mm} \times 0.035 \text{ mm}$  in size with an adjacent distance of  $15 \text{ mm}$  between each electrode. Objects can approach the sensor on an arbitrary path and move randomly around in front of the sensor plane. Depending on the configuration a complete measurement matrix  $n \times n$  can be obtained per measurement cycle with the evaluation circuit. Details on the electronic hardware can be found in [11].

### D. Fast Bayesian Reconstruction

OFOA is a type of fast Bayesian reconstruction techniques addressing the quality criteria of the reconstructed image by minimizing the mean square error between the reconstructed conductivity value  $\hat{\sigma}_l$  and the true conductivity value  $\sigma_l$ . The optimal reconstruction function  $\mathbf{f}_{i,\text{opt}}$  for the  $i^{\text{th}}$  reconstruction element out of a set of  $\Phi$  reconstruction functions is given by

$$\mathbf{f}_{i,\text{opt}} = \arg \min_{\mathbf{f}_i \in \Phi} E \left\{ (\hat{\sigma}_l - \sigma_l)^2 \right\} \quad (1)$$

The expected value  $E \{ \}$  of the leakage conductivity  $\sigma_l$  conditioned on the measurements is a solution of Eq. 1, which can be approximated by a linear function of the measurement vector. This is done to increase the reconstruction speed to fulfill the real-time capabilities of the reconstruction algorithm.

$$\hat{\sigma}_l \text{ MMSE} = E \{ \sigma_l | \mathbf{y} \} \approx W_{\sigma_l} \mathbf{y} + B_{\sigma_l} \quad (2)$$

The optimal solution for  $W_{\sigma_l}$  and  $B_{\sigma_l}$  is obtained with

$$W_{\sigma_l} = C_{\sigma_l} C_{YY}^{-1} \quad (3)$$

$$B_{\sigma_l} = \bar{\sigma}_l - W_{\sigma_l} \bar{\mathbf{y}} \quad (4)$$

where  $C_{\sigma_l}$  is the cross-covariance matrix between the measurements and leakage conductivity,  $C_{YY}$  is the auto-covariance matrix of the measurements,  $\bar{\sigma}_l$  is the expected leakage conductivity according to the prior probability and  $\bar{\mathbf{y}}$  is the expected value of the measurements [9].

### E. Artifacts and Artifacts Reduction

To eliminate this artifacts caused by OFOA we apply the Box-Cox transformation [10] given by

$$\sigma_{l_i}^{(\lambda)} = \begin{cases} \frac{\sigma_{l_i}^\lambda - 1}{\lambda} & \lambda \neq 0 \\ \log \sigma_{l_i} & \lambda = 0 \end{cases} \quad (5)$$

to the leakage conductivity values sampled from the prior distribution. For our setup the optimal values of the transformation parameter is  $\lambda = 0.4$  used for all objects made of conductive material. This is obtained using a grid search technique.

### F. Simulations - Forward Model

The forward problem is solved as 3D model whereas the 2D reconstruction images are the cross section (x-y plane) of the model. To avoid errors introduced by remeshing the ROI while the object is repositioned, the simulation is done twice. First, the problem is solved for  $\varepsilon_r = 1$ . To model the coupling to ground for objects with high conductivity it is sufficient to set the boundaries of the object to the desired value. In the second case, the problem is solved while the surface of the object with a diameter  $d_s = 40 \text{ mm}$  is set to ground.

### G. Detector Design

A hypothesis test is applied to each reconstructed element to detect and estimate the position of an object in the ROI. The hypothesis test can be formally written as

$$\begin{aligned} H_0 &: \text{No Object is present at position } P \\ H_1 &: \text{Object is present at position } P. \end{aligned} \quad (6)$$

which can be rewritten to

$$\begin{aligned} H_0 &: \nexists \sigma_{l_i} \in K \mid \sigma_{l_i} > 0 \\ H_1 &: \exists \sigma_{l_i} \in K \mid \sigma_{l_i} > 0 \end{aligned} \quad (7)$$

where  $\sigma_l$  is the leakage conductivity and  $K$  includes all elements in a surrounding neighborhood (safety margin) of point  $P$ . The null hypothesis is rejected in case the evidence is strong enough to ensure a low false alarm rate. The alternative hypothesis  $H_1$  is accepted, i.e.  $\hat{\sigma}_l > \gamma$  when  $H_0$  is true, if the probability

$$P(\hat{\sigma}_l > \gamma \mid H_0) \leq \alpha \quad (8)$$

with the threshold  $\gamma = \sigma_{l_{th}}$ . The confidence level  $\alpha$  is set to 5%. The PDF  $f(\hat{\sigma}_l | H_0)$  can be approximated utilizing the histogram from the reconstructed elements under the condition of  $H_0$  sampled from an assumed prior distribution. Consequently, the CDF can be found to obtain  $\sigma_{l_{th}}$  and the Receiver Operator Characteristic (ROC) can be generated to evaluate the detection performance.

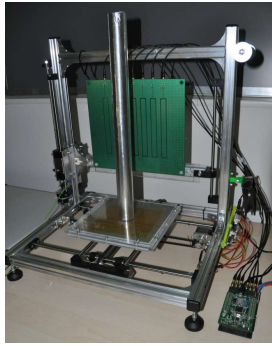


Fig. 3. ECT system test bench comprising a planar sensor front end, a sample object (aluminum rod) on a 2D translation stage connected via coaxial cables to the measurement hardware.

#### IV. EXPERIMENTAL SETUP

The experiments are conducted on a test bench (see Fig. 3) using a 2D translation stage to precisely move the rods in front of the sensor plane in an area of  $x = 0 - 0.2\text{m}$  and  $y = 0 - 0.1\text{m}$ . This area is defined as the ROI, where the reconstruction of the 2D images takes place. The rod is made of aluminum, with a diameters of  $d_s = 40\text{mm}$ . The leakage conductivity was assumed to be  $\sigma_l = 1$ . The conductive objects are well coupled to ground in the experimental setup and an offset calibration is used.

#### V. EXPERIMENTAL RESULTS

Fig. 4 shows snapshots from the online reconstruction and detection with objects moved around using the translation stage in the ROI. The algorithm run-time is less than 1 ms to obtain

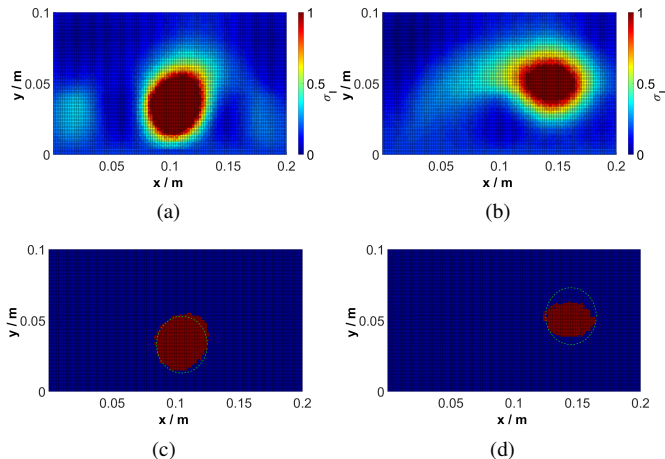


Fig. 4. Reconstruction results (a), (b) of the leakage conductivity and detection results (c), (d) of the hypothesis test based on the reconstruction results in the ROI for a stick with  $\sigma_l = 1$  and  $d = 40\text{mm}$ . Detection results: red pixels depict elements, where an object is detected; at blue pixels no object is detected. The true position of the object is illustrated by a dashed green line. (a) The region of high leakage conductivity is clearly delimited and also only marginal artifacts occur at the bottom left and right side of the image. (c) The object in the ROI is clearly detected. In addition, also the position of the object matches well with the true position. (b) The delimitation of the region of the high leakage conductivity gets blurred with increasing distance to the electrodes. (d) The presence of an object in ROI can be detected. However, the size of the detected object is slightly smaller than the real object.

a new detection result. The results show that the simulation model of Sec. III-F is usable to reconstruct the leakage conductivity. Moreover, an object detection can be done based on the obtained reconstruction images. The reconstruction images (e.g. Fig. 4(a)) achieve low artifacts for conductive objects in the ROI further processed for object detection. In regions with lower sensitivity (boundary of ROI) the position accuracy of the detected object decreases and the objects starts to vanish (see 4(b)). The detection range strongly depends on the design of the electrodes, the signal to noise ratio achieved with the measurement setup and the measurement rate. Thus, it can be adopted according to the needs of a certain application.

#### VI. CONCLUSION

The feasibility to combine leakage conductivity images of an ECT system together with hypothesis testing to detect the presence/absence together with a position estimation of conductive objects in the ROI is presented. Considering the leakage effect in the reconstruction algorithm, extends the applicability to conductive materials and objects with a strong coupling to distant ground. The proposed light-weight signal processing chain and detection algorithm offers realtime capability and extends the applicability of this technology in particular with respect to mobile applications.

#### REFERENCES

- [1] W. Yang and L. Peng, "Image reconstruction algorithms for electrical capacitance tomography," *Meas. Sci. Technol.*, vol. 14, no. 1, pp. R1–R13, January 2003.
- [2] S. Mühlbacher-Karrer and H. Zangl, "Object detection based on electrical capacitance tomography," in *IEEE Sensors Applications Symposium*, 2015.
- [3] T. Schlegl, T. Bretterklieber, S. Muehlbacher-Karrer, and H. Zangl, "Simulation of the leakage effect in capacitive sensors," *International Journal on Smart Sensing and Intelligent Systems*, vol. 7, no. 4, pp. 1579 – 1594, December 2014.
- [4] T. Schlegl, M. Neumayer, S. Muehlbacher-Karrer, and H. Zangl, "A pretouch sensing system for a robot grasper using magnetic and capacitive sensors," *IEEE transactions on instrumentation and measurement*, p. in press, 2013.
- [5] C. Xie, S. Huang, B. Hoyle, R. Thorn, C. Lenn, D. Snowden, and M. Beck, "Electrical capacitance tomography for flow imaging: system model for development of image reconstruction algorithms and design of primary sensors," *Circuits, Devices and Systems, IEE Proceedings G*, vol. 139, no. 1, pp. 89–98, Feb 1992.
- [6] M. Soleimani, P. K. Yalavarthy, and H. Dehghani, "Helmholtz-type regularization method for permittivity reconstruction using experimental phantom data of electrical capacitance tomography," *Instrumentation and Measurement, IEEE Transactions on*, vol. 59, no. 1, pp. 78–83, 2010.
- [7] H. Zangl and S. Mühlbacher-Karrer, "Artefact reduction in fast Bayesian inversion in electrical tomography," in *International IGTE Symposium*, Graz, 09 2014.
- [8] J. P. Kaipio and E. Somersalo, *Statistical and Computational Inverse Problems*. Applied Mathematical Sciences, Springer Verlag New York, Inc., 2004.
- [9] H. Zangl, D. Watzenig, G. Steiner, A. Fuchs, and H. Wegleiter, "Non-iterative reconstruction for electrical tomography using optimal first and second order approximations," in *5th World Congress on Industrial Process Tomography*, Bergen, Norway, September 3-6, 2007.
- [10] G. E. Box and D. R. Cox, "An analysis of transformations," *Journal of the Royal Statistical Society. Series B (Methodological)*, pp. 211–252, 1964.
- [11] T. Schlegl and H. Zangl, "Sensor interface for multimodal evaluation of capacitive sensors," *Journal of Physics: Conference Series*, vol. 450, no. 1, p. 012018, 2013.